World ocean heat content and thermosteric sea level change (0–2000 m), 1955–2010

S. Levitus,[1] J. I. Antonov,[2] T. P. Boyer,[1] O. K. Baranova,[1] H. E. Garcia,[1] R. A. Locarnini,[1] A. V. Mishonov,[1] J. R. Reagan,[1] D. Seidov,[1] E. S. Yarosh,[1] and M. M. Zweng[1]

Received 26 January 2012; revised 11 April 2012; accepted 16 April 2012; published 17 May 2012.

[1] We provide updated estimates of the change of ocean heat content and the thermosteric component of sea level change of the 0–700 and 0–2000 m layers of the World Ocean for 1955–2010. Our estimates are based on historical data not previously available, additional modern data, and bathythermograph data corrected for instrumental biases. We have also used Argo data corrected by the Argo DAC if available and used uncorrected Argo data if no corrections were available at the time we downloaded the Argo data. The heat content of the World Ocean for the 0–2000 m layer increased by $24.0 \pm 1.9 \times 10^{22}$ J (±2S.E.) corresponding to a rate of 0.39 W m^{-2} (per unit area of the World Ocean) and a volume mean warming of 0.09°C. This warming corresponds to a rate of 0.27 W m^{-2} per unit area of earth's surface. The heat content of the World Ocean for the 0–700 m layer increased by $16.7 \pm 1.6 \times 10^{22}$ J corresponding to a rate of 0.27 W m^{-2} (per unit area of the World Ocean) and a volume mean warming of 0.18°C. The World Ocean accounts for approximately 93% of the warming of the earth system that has occurred since 1955. The 700–2000 m ocean layer accounted for approximately one-third of the warming of the 0–2000 m layer of the World Ocean. The thermosteric component of sea level trend was $0.54 \pm .05$ mm yr^{-1} for the 0–2000 m layer and $0.41 \pm .04$ mm yr^{-1} for the 0–700 m layer of the World Ocean for 1955–2010. **Citation:** Levitus, S., et al. (2012), World ocean heat content and thermosteric sea level change (0–2000 m), 1955–2010, *Geophys. Res. Lett.*, *39*, L10603, doi:10.1029/2012GL051106.

1. Introduction

[2] We have previously reported estimates of the variability of ocean heat content (OHC) of the World Ocean to a depth of 3000 m [*Levitus et al.*, 2000]. Here we present estimates for the upper 2000 m of the World Ocean with additional historical and modern data [*Levitus et al.*, 2005a, 2005b; *Boyer et al.*, 2009] using running pentadal (5-year) temperature analyses [*Levitus et al.*, 2000]. A lack of high-quality CTD and reversing thermometer data at depths exceeding 2000 m in recent years precludes us from producing recent analyses for deeper depths.

[3] We use the term "ocean heat content" as opposed to "ocean heat content anomaly" used by some authors because "ocean heat content" is an anomaly by definition. OHC is always computed with a reference mean subtracted out from each temperature observation. Otherwise the OHC computation depends on the temperature scale used.

[4] The importance of the variability of the total heat content of the world ocean can hardly be underestimated. *Levitus et al.* [2001] documented quantitatively that global ocean heat content is the major term in earth's heat balance.

2. Data and Method

[5] We use data from the World Ocean Database 2009 [*Boyer et al.*, 2009] plus additional data processed through the end of 2010 (http://www.nodc.noaa.gov).

[6] Argo profiling float data that have been corrected for systematic errors provide data through a nominal depth of 1750–2000 m for the post-2004 period on a near-global basis. We have used data that were available as of January 2011. Many of these data have been corrected by the Argo delayed-mode quality control teams. If Argo data have not been corrected at the time we downloaded these data we still used them. Unlike salinity data from profiling floats, temperature data do not appear to have significant drift problems associated with them. It is our understanding that problems with profiling floats identified by *Barker et al.* [2011] have for the most part been corrected. Also, we believe that our quality control procedures [*Boyer et al.*, 2009; *Boyer and Levitus*, 1994] have eliminated most remaining egregious problems. Typically most Argo floats in our present database reach a maximum observed depth of 1970 m. Thus, these profiles only extend down to the 1750 m standard depth level of our analyses. Our temperature anomaly fields could be considered to be more representative of the 0–1750 m layer of the World Ocean however we have compared the OHC1750 and OHC2000 and find no difference between them. We hope to acquire additional deep ocean data from research cruises so we have opted to present results for the 0–2000 m layer.

[7] We apply corrections for instrumental offsets of expendable bathythermographs (XBT) and mechanical bathythermographs (MBT) found by *Gouretski and Koltermann* [2007] as described by *Levitus et al.* [2009]. XBT profiles are excluded from our computations if they lack the metadata needed to correct drop rates. This is approximately 3.8% of all XBT profiles that are in the World Ocean Database.

[8] From every observed one-degree mean temperature value at every standard depth level we subtract off a

[1]National Oceanographic Data Center, NOAA, Silver Spring, Maryland, USA.
[2]UCAR Project Scientist, National Oceanographic Data Center, Silver Spring, Maryland, USA.

Corresponding author: S. Levitus, National Oceanographic Data Center, NOAA, E/OC5, 1315 East-West Hwy., Silver Spring, MD 20910, USA. (sydney.levitus@noaa.gov)

0094-8276/12/2012GL051106

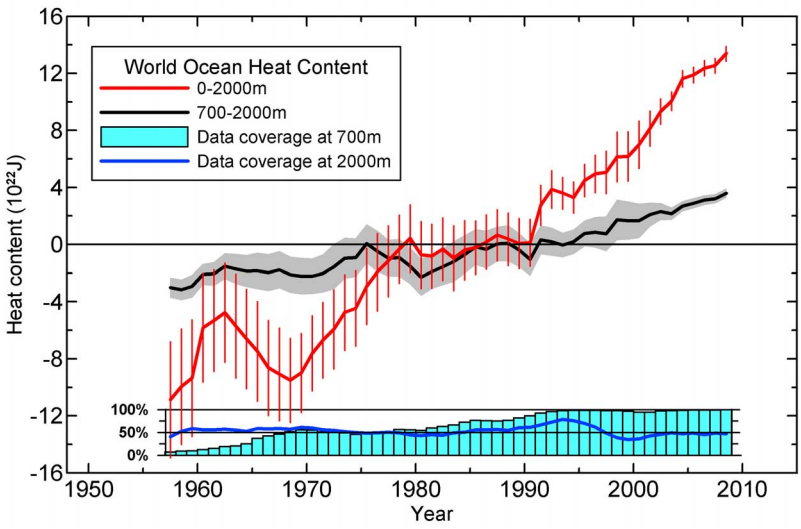

Figure 1. Time series for the World Ocean of ocean heat content (10^{22} J) for the 0–2000 m (red) and 700–2000 m (black) layers based on running pentadal (five-year) analyses. Reference period is 1955–2006. Each pentadal estimate is plotted at the midpoint of the 5-year period. The vertical bars represent +/−2.*S.E. about the pentadal estimate for the 0–2000 m estimates and the grey-shaded area represent +/−2.*S.E. about the pentadal estimate for the 0–700 m estimates. The blue bar chart at the bottom represents the percentage of one-degree squares (globally) that have at least four pentadal one-degree square anomaly values used in their computation at 700 m depth. Blue line is the same as for the bar chart but for 2000 m depth.

climatological value. For this purpose we use the monthly climatological fields of temperature from *Locarnini et al.* [2010]. Then we composite all anomaly values in each one-degree square by five-year running compositing periods. Next the same objective analysis procedure used by *Locarnini et al.* [2010] is applied to these gridded, composited anomaly values and a global, gridded field with temperature anomaly values defined in every one-degree square is produced for each standard depth level. To compute heat content at each gridpoint the specific heat and density were computed using annual climatological values of temperature and salinity from *Locarnini et al.* [2010] and *Antonov et al.* [2010]. We use a first-guess field of zero for our anomaly field computations. This is a conservative but we think appropriate procedure given the lack of data in some regions and some time periods. There are alternative methods for interpolation or as some investigators refer to it "infilling". For example *Gille* [2008] used a basin or global mean trend in data void areas. *Domingues et al.* [2008] used basis functions of near-global sea level determined from satellite altimeter data for 1993–2006 and historical observations of the steric component of sea level to derive near global ocean heat content fields. Each of these methods has deficiencies. For example the basis functions used by *Domingues et al.* [2008] may be changing with time. We computed decadal monthly means by averaging all data within each month for decadal periods beginning with 1955–1964 and then averaging these decadal climatological monthly means to compute the long-term climatological monthly mean (1955–2006) at each gridpoint. This is necessary in particular because of the large amount of Argo profiling float data introduced to the observing system in recent years which can bias climatologies to the Argo sampling period. This change made no difference in the time series of northern hemisphere ocean heat content but did make a small difference in the southern hemisphere ocean heat content.

3. Global and Basin OHC Estimates

[9] Figure 1 shows the 0–2000 m and 700–2000 m OHC pentadal time series for the World Ocean. We will denote the OHC integrated to a particular depth as OHCXXXX in which "XXXX" is the maximum depth of vertical integration in meters. The global linear trend of OHC2000 is 0.43×10^{22} J yr^{-1} for 1955–2010 which corresponds to a total increase in heat content of $24.0 \pm 1.9 \times 10^{22}$ J (±2S.E.), and a mean increase of temperature of 0.09°C. This represents a rate of 0.39 W m^{-2} per unit area of the World Ocean and a rate of 0.27 W m^{-2} per unit area of the earth's surface. The corresponding total OHC700 increase for the same period is $16.7 \pm 1.6 \times 10^{22}$ J that represents a rate of 0.27 W m^{-2} per unit area of the World Ocean. The linear trends account for 93 and 91 per cent of the variability of the OHC2000 and OHC700 World Ocean time series respectively. The standard error of the mean (S.E.) for each pentadal estimate is computed as described in Text S1 in the auxiliary material.[1] Figure 1 shows that the 700–2000 m layer is responsible for approximately one third of the total warming of the 0–2000 m layer. The blue bar chart at the bottom represents the percentage of one-degree squares (globally) that have at least four pentadal one-degree square anomaly values used to compute one-degree square values at 700 m depth. The blue line is the same quantity as for the bar chart but for 2000 m depth. Figure S1 displays OHC2000 estimates for each major ocean basin. Figure S2 is similar to Figure S1 but shows the OHC700 time series.

[1]Auxiliary materials are available in the HTML. doi:10.1029/2012GL051106.

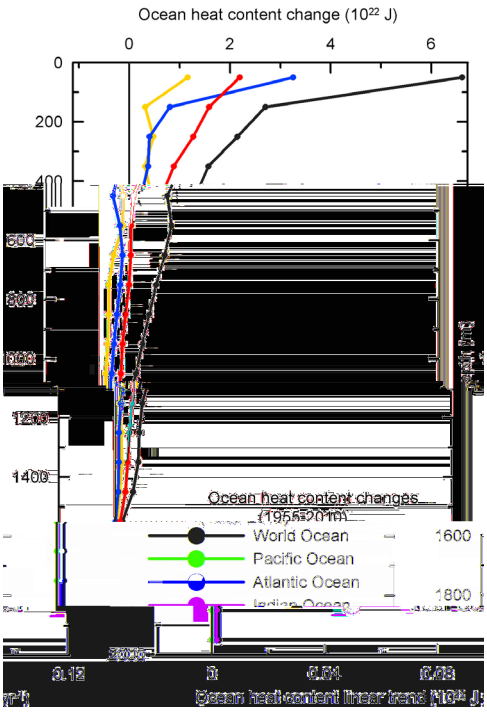

Figure 2. Linear trend and total increase of ocean basin heat content based on the linear trend of global and individual basins as a function of depth (0–2000 m) for 100 m thick layers.

[10] Figure 2 shows the linear trend and total increase of heat content for 1955–2010 of global and basin heat content as a function of depth (0–2000 m) for 100 m layers. We computed basin time series of OHC for 100 m-thick layers from 0 to1500 m and 250 m-thick layers between 1500 m and 2000 m. Then the linear trends for each time series were computed. For the deepest two layers (1500–1750 m and 1750–2000 m) we added the linear trends of 1500–1750 m and 1750–2000 m layers to get the total change of the 1500–2000 m layer and divided that total change by five (the number of 100 m-thick layers between 1500 m and 2000 m) to plot in Figure 2. Warming is surface intensified in all basins. In the 0–100 m layer the Pacific exhibits the largest total increase. Below the 100 m layer the Atlantic exhibits the largest increase of all ocean basins at all layers down to 2000 m depth. Figure S3 shows the percent variance accounted for by the linear trend in each layer of the basins in Figure 2. In the Atlantic Ocean the linear trend has accounted for at least 60% of the variance at all layers to depths just exceeding 1500 m. The Pacific shows percent variance contributions near or exceeding 60% in the 0–100 m layer and between 500 and 1100 m depth. The Indian Ocean differs considerably and shows the greatest percent variance contributed by the linear trend in the 0–100 m, 200–500 m, and 1100–1500 m layers.

4. Zonally-Integrated OHC Pentadal Difference Estimates and Trends

[11] Figure 3 shows the linear trend of the zonally integrated OHC2000 fields for the 1955–2010 period as a function of latitude for the World Ocean and individual ocean basins. At nearly every latitude the World Ocean has warmed. Relative extrema in the linear trend of OHC occur at several latitudes in each basin. Some of these extremes coincide between the three basins and others do not. Figure S4 shows the percent variance accounted for by the linear trends shown in Figure 3. Generally the percent variance accounted for is relatively high in the vicinity of the extrema observed in Figure 3. In the Atlantic the percent

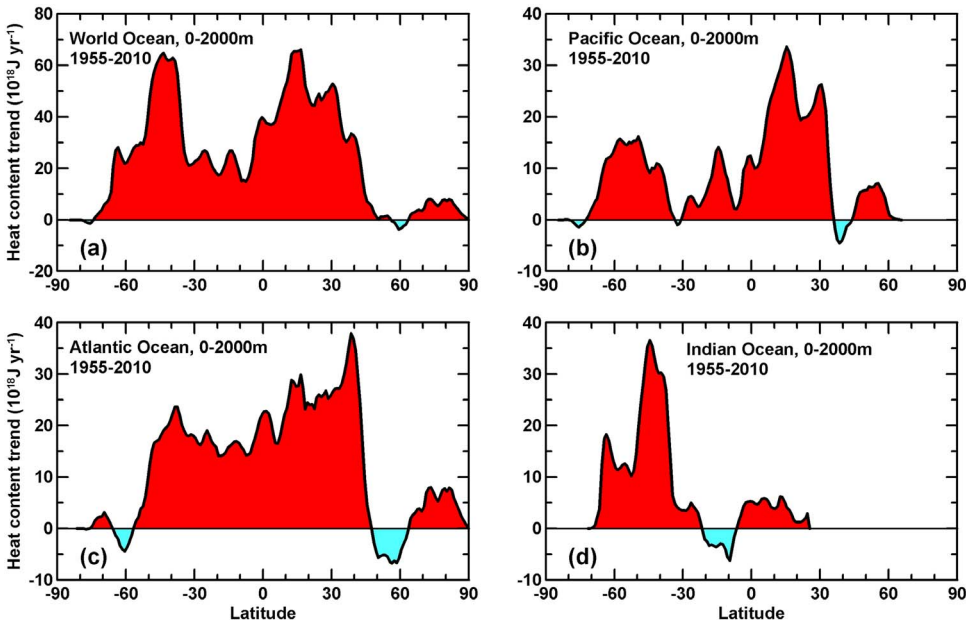

Figure 3. Linear trend (10^{18} J yr^{-1}) (1955–1959) to (2006–2010) in zonally integrated ocean heat content for the World Ocean and individual ocean basins as function of latitude for the 0–2000 m layer. Red indicates a positive trend and blue a negative trend.

variance exceeds 60% at nearly all latitudes between 50°S and 40°N and exceeds 80% in much of this region.

[12] Figure S5 shows the zonally integrated OHC700 and OHC2000 difference fields for the (2006–2010) minus (1955–1959) pentads as a function of latitude. As indicated by Figure 3, warming is nearly ubiquitous at all latitudes. In addition heat has been stored in the 700–2000 m layer. Previous evidence of the role played by the 700–2000 m layer in storing heat particularly in the southern hemisphere was given by *Levitus et al.* [2005a] and *Cai et al.* [2010]. Cai et al. used ensemble mean results from seventeen AOGCMs (Atmosphere-Ocean General Circulation Models) that were forced by the increase of atmospheric greenhouse gases (from the Third Coupled Model Intercomparison Project (CMIP3) in support of the IPCC AR4). They found relatively "fast, deep ocean warming in the midlatitude" band of the southern hemisphere which agrees with our observational results. Furthermore they found that "Counterintuitively, the net heat required for warming in this midlatitude band is largely derived from surface heat fluxes south of 50°S, where the changes are an order of magnitude greater than that over the 35°–50°S midlatitude band".

5. Global Distribution of Ocean Heat Storage

[13] We define ocean heat storage as the time derivative of OHC. Figure S6 shows the linear trend of global geographical distribution of heat storage for the 0–2000 m layer for 1955–2010. Heat storage is generally positive as would be expected from Figure 3. A notable exception is the subarctic gyre of the North Atlantic Ocean. This is due to multidecadal variability in ocean temperature anomalies that we have observed in this region. *Hatún et al.* [2005] noted that the subarctic Atlantic Ocean began warming in 1995 after a period of cooling that began in the 1970s. We document these changes in more detail in J. I. Antonov et al. (Multidecadal variability of temperature and salinity of the North Atlantic subarctic gyre, manuscript in preparation, 2012). Figure S7 shows the percent variance accounted for by the linear trend shown in Figure S6. The 0–700 m global ocean heat storage is given in Figure S8 and the percent variance account for by the trend is given by Figure S9. Tables S1 and S2 provide ocean heat content estimates and calculation discussed in this paper in tabular form.

6. Contributions to Ocean Heat Content From Regions Deeper Than 2000 m Depth

[14] Although observational data are relatively sparse from depths exceeding 2000 m in the World Ocean, several recent studies have appeared that estimate the change in ocean heat content in this layer. *Purkey and Johnson* [2010] quantified abyssal global and deep Southern Ocean temperature trends between the 1990s and 2000s with CTD data from research cruises. *Kouketsu et al.* [2011] assimilated temperature and salinity data into an ocean general circulation model (OGCM) and found a global increase of 0.8×10^{22} J decade^{-1} for depths exceeding 3000 m for the 1990s to 2000s. *Kawano et al.* [2010] estimated that for the Pacific Ocean the increase in ocean "heat content below 3000 m was about 5% of the ocean-wide increase" between 1999 and 2007.

7. Thermosteric Sea Level

[15] We update our earlier estimates of the thermosteric component of global sea level rise (TCSL) [*Antonov et al.*, 2005]. For 1955–2010 the TCSL has increased at rates of 0.54 mm yr^{-1} and 0.41 mm yr^{-1} for the 0–2000 m and 0–700 m layers respectively. The 0–700 m value is approximately 25% larger than our earlier estimate which most likely can be attributed to additional data now available for use in this study. The global and basin time series of TCSL are shown in Figures S10 (0–2000 m) and S11 (0–700 m). Table S3 provides TCSL rates in tabular form.

[16] For comparison we note that a total global sea level rise of approximately 1.6–1.8 mm yr^{-1} had been estimated on the basis of tide gauge data for most of the twentieth century. More recently there has been acceleration in sea level rise and both tide gauges and satellite altimetry estimate a rise of sea level of approximately 3.1 mm yr^{-1} since 1991.

8. Discussion

[17] One important result presented here is that each major ocean basin has warmed at nearly all latitudes. A net warming has occurred despite interannual to decadal variability of the ocean associated with phenomenon such as the El Niño-Southern Oscillation, the Pacific Decadal Oscillation, and the North Atlantic Oscillation as well as other such phenomenon. The fact that relative extremes of OHC are a function of latitude and in some cases are at different latitudes in each major ocean basin indicates different ocean, or ocean-atmosphere, responses to the common forcing of the observed increase in greenhouse gases in earth's atmosphere occurred. Although carbon dioxide is well-mixed in the atmosphere, the response of earth's climate system to increasing atmospheric greenhouse gases is not simple [*Cai et al.*, 2010]. Work by *Lee et al.* [2011] documents interbasin exchange of heat that is of possible relevance to both internal and anthropogenic variability of the world ocean.

[18] Using model simulations based on AOGCM simulations, *Dommenget* [2009] concluded that "continental warming due to anthropogenic forcing (e.g., the warming at the end of the last century or future climate change scenarios) is mostly (80%–90%) indirectly forced by the contemporaneous ocean warming, not directly by local radiative forcing." Thus even if greenhouse gas emissions were halted today than regardless of the residence time of the carbon dioxide in today's atmosphere, the ocean would continue to heat the atmosphere [*Wetherald et al.*, 2001] .

[19] One feature of our results is that the previous multidecadal increase in OHC700 that we have reported [*Levitus et al.*, 2009] (updated estimates available online at http://www.nodc.noaa.gov) leveled off during the past several years. This leveling is not as pronounced in our OHC2000 estimates indicating that heat is being stored in the 700–2000 m layer as we have shown here. We also note that our new yearly OHC2000 time series (not shown here) indicate that the positive trend in this quantity continues

through 2011 although with interannual and interseasonal variability apparent.

[20] We emphasize that despite the surface intensification of the observed ocean warming, subsurface layers make a substantial contribution to the increase in OHC. Heat may have been stored at ocean depths exceeding 2000 m during the observational period we are studying and may be of significance for earth's heat balance. We simply do not have enough in situ CTD or reversing thermometer data from depths exceeding 2000 m available to ascertain if there is a contribution from this layer. If the results of *Kouketsu et al.* [2011] are correct, this would mean a contribution of 1.6×10^{22} J from the ocean region in the 3000 m-bottom layer. However a reduction of global ocean heat storage may result from the increase of sulfur in earth's atmosphere due to increased burning of coal as well as decreased solar radiation and changes in the state of ENSO as recently suggested by *Kaufmann et al.* [2011]. Observed changes in stratospheric water vapor [*Solomon et al.*, 2010] and stratospheric aerosols [*Solomon et al.*, 2011] may also have contributed. *Church et al.* [2011] discussed these factors in a study of the variability of ocean heat content and sea level.

[21] We have estimated an increase of 24×10^{22} J representing a volume mean warming of 0.09°C of the 0–2000 m layer of the World Ocean. If this heat were instantly transferred to the lower 10 km of the global atmosphere it would result in a volume mean warming of this atmospheric layer by approximately 36°C (65°F). This transfer of course will not happen; earth's climate system simply does not work like this. But this computation does provide a perspective on the amount of heating that the earth system has undergone since 1955.

[22] All data and pentadal analyses used in this study as well as the yearly and seasonal gridded heat content fields are freely available at (http://www.nodc.noaa.gov/OC5/indprod.html). This is in accordance with IPCC, ICSU, IOC, and national data policies of many countries.

[23] **Acknowledgments.** This work was supported by the NOAA Climate Program Office. We thank the scientists, technicians, data center staff, and data managers for their contributions of data to the IOC/IODE and ICSU/World Data Center system which has allowed us to compile the database used in this work. We also thank our colleagues at NODC for data processing work and our colleagues at the NODC Ocean Climate Laboratory for their work in constructing the *World Ocean Database* which made this work possible. We appreciate review of our manuscript by Charles Sun and anonymous reviewers. The Argo profiling float data used in this study were made freely available by the International Argo Project and the national initiatives that contribute to it (http://www.argo.net). Argo is a pilot programme of the Global Ocean Observing System. The views, opinions, and findings contained in this report are those of the authors and should not be construed as an official NOAA or U.S. Government position, policy, or decision.

[24] The Editor thanks two anonymous reviewers for assisting with the evaluation of this paper.

References

Antonov, J. I., S. Levitus, and T. P. Boyer (2005), Thermosteric sea level rise, 1955–2003, *Geophys. Res. Lett.*, *32*, L12602, doi:10.1029/2005GL023112.

Antonov, J. I., D. Seidov, T. P. Boyer, R. A. Locarnini, A. V. Mishonov, H. E. Garcia, O. K. Baranova, M. M. Zweng, and D. R. Johnson (2010), *World Ocean Atlas 2009*, vol. 2, *Salinity*, *NOAA Atlas NESDIS*, vol. 69, edited by S. Levitus, 184 pp., NOAA, Silver Spring, Md.

Barker, P. M., J. R. Dunn, C. M. Domingues, and S. E. Wijffels (2011), Pressure sensor drifts in Argo and their impacts, *J. Atmos. Oceanic Technol.*, *28*, 1036–1049, doi:10.1175/2011JTECHO831.1.

Boyer, T. P., and S. Levitus (1994), Quality control of oxygen, temperature and salinity data, *NOAA Tech. Rep. 81*, 65 pp., Natl. Oceanogr. Data Cent., Silver Spring, Md.

Boyer, T. P., et al. (2009), *World Ocean Database 2009*, vol. 1, *Introduction*, *NOAA Atlas NESDIS*, vol. 66, edited by S. Levitus, 219 pp., NOAA, Silver Spring, Md.

Cai, W. J., T. Cowan, S. Godfrey, and S. Wijffels (2010), Simulations of processes associated with the fast warming rate of the southern midlatitude ocean, *J. Clim.*, *23*, 197–206, doi:10.1175/2009JCLI3081.1.

Church, J. A., N. J. White, L. F. Konikow, C. M. Domingues, J. G. Cogley, E. Rignot, J. M. Gregory, M. R. van den Broeke, A. J. Monaghan, and I. Velicogna (2011), Revisiting the Earth's sea-level and energy budgets from 1961 to 2008, *Geophys. Res. Lett.*, *38*, L18601, doi:10.1029/2011GL048794.

Domingues, C. M., J. A. Church, N. J. White, P. J. Gleckler, S. E. Wijffels, P. M. Barker, and J. R. Dunn (2008), Improved estimates of upper-ocean warming and multi-decadal sea-level rise, *Nature*, *453*, 1090–1093, doi:10.1038/nature07080.

Dommenget, D. (2009), The ocean's role in continental climate variability and change, *J. Clim.*, *22*, 4939–4952, doi:10.1175/2009JCLI2778.1.

Gille, S. T. (2008), Decadal-scale trends in the Southern Hemisphere, *J. Clim.*, *21*, 4749–4765, doi:10.1175/2008JCLI2131.1.

Gouretski, V., and K. P. Koltermann (2007), How much is the ocean really warming?, *Geophys. Res. Lett.*, *34*, L01610, doi:10.1029/2006GL027834.

Hatún, H., A. B. Sando, H. Drange, B. Hansen, and H. Valdimarsson (2005), Influence of the Atlantic subpolar gyre on the thermohaline circulation, *Science*, *309*, 1841–1844, doi:10.1126/science.1114777.

Kaufmann, R. K., H. Kauppi, M. L. Mann, and J. H. Stock (2011), Reconciling anthropogenic climate change with observed temperature 1998–2008, *Proc. Natl. Acad. Sci. U. S. A.*, *108*, 11,790–11,793, doi:10.1073/pnas.1102467108.

Kawano, T., T. Doi, H. Uchida, S. Kouketsu, M. Fukasawa, Y. Kawai, and K. Katsumata (2010), Heat content change in the Pacific Ocean between the 1990s and 2000s, *Deep Sea Res., Part II*, *57*(13–14), 1141–1151, doi:10.1016/j.dsr2.2009.12.003.

Kouketsu, S., et al. (2011), Deep ocean heat content changes estimated from observation and reanalysis product and their influence on sea level change, *J. Geophys. Res.*, *116*, C03012, doi:10.1029/2010JC006464.

Lee, S.-K., W. Park, E. van Sebille, M. O. Baringer, C. Wang, D. B. Enfield, S. G. Yeager, and B. P. Kirtman (2011), What caused the significant increase in Atlantic Ocean heat content since the mid-20th century?, *Geophys. Res. Lett.*, *38*, L17607, doi:10.1029/2011GL048856.

Levitus, S., J. Antonov, T. P. Boyer, and C. Stephens (2000), Warming of the world ocean, *Science*, *287*, 2225–2229, doi:10.1126/science.287.5461.2225.

Levitus, S., J. L. Antonov, J. Wang, T. L. Delworth, K. W. Dixon, and A. J. Broccoli (2001), Anthropogenic warming of Earth's climate system, *Science*, *292*, 267–270, doi:10.1126/science.1058154.

Levitus, S., J. Antonov, and T. Boyer (2005a), Warming of the world ocean, 1955–2003, *Geophys. Res. Lett.*, *32*, L02604, doi:10.1029/2004GL021592.

Levitus, S., S. Sato, C. Maillard, N. Mikhailov, P. Caldwell, and H. Dooley (2005b), Building ocean profile-plankton databases for climate and ecosystem research, *NOAA Tech. Rep. NESDIS 117*, 29 pp., NOAA, Silver Spring, Md.

Levitus, S., J. I. Antonov, T. P. Boyer, H. E. Garcia, R. A. Locarnini, A. V. Mishonov, and H. E. Garcia (2009), Global ocean heat content 1955–2008 in light of recently revealed instrumentation problems, *Geophys. Res. Lett.*, *36*, L07608, doi:10.1029/2008GL037155.

Locarnini, R. A., A. V. Mishonov, J. I. Antonov, T. P. Boyer, and H. E. Garcia (2010), *World Ocean Atlas 2009*, vol. 1, *Temperature*, *NOAA Atlas NESDIS*, vol. 68, edited by S. Levitus, 184 pp., NOAA, Silver Spring, Md.

Purkey, S. G., and G. C. Johnson (2010), Warming of global abyssal and deep Southern Ocean waters between the 1990s and 2000s: Contributions to global heat and sea level rise budgets, *J. Clim.*, *23*, 6336–6351, doi:10.1175/2010JCLI3682.1.

Solomon, S., K. H. Rosenlof, R. W. Portmann, J. S. Daniel, S. M. Davis, T. J. Sanford, and G.-K. Plattner (2010), Contributions of stratospheric water vapor to decadal changes in the rate of global warming, *Science*, *327*, 1219–1223, doi:10.1126/science.1182488.

Solomon, S., J. S. Daniel, R. R. Neely III, J. P. Vernier, E. G. Dutton, and L. W. Thomason (2011), The persistently variable "background" stratospheric aerosol layer and global climate change, *Science*, *333*, 866–870, doi:10.1126/science.1206027.

Wetherald, R. T., R. J. Stouffer, and K. W. Dixon (2001), Committed warming and its implications for climatic change, *Geophys. Res. Lett.*, *28*, 1535–1538, doi:10.1029/2000GL011786.

Auxiliary material for:

World ocean heat content and thermosteric sea level change (0-2000 m), 1955-2010

By Levitus et al.

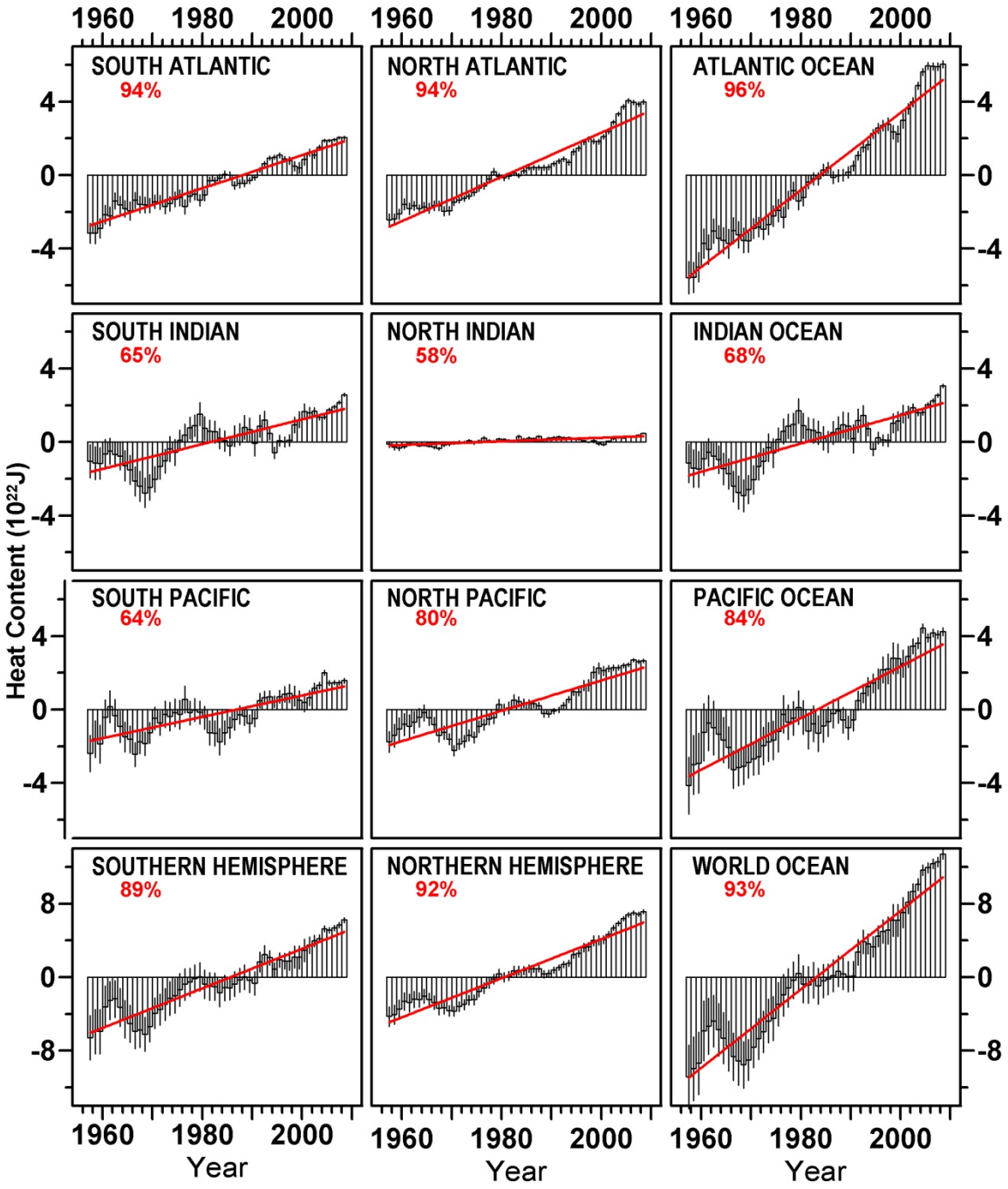

Figure S1. Time series of ocean heat content (10^{22}J) for the 0-2000 m layer for the major ocean basins based on running pentadal analyses. Each pentadal estimate is plotted at the midpoint of the 5-year period. The vertical bars represent +/- 2.*S.E. about the pentadal estimate. The linear trend line and the percent variance accounted for by the linear trend are shown in red on each panel. Reference period is 1955-2006.

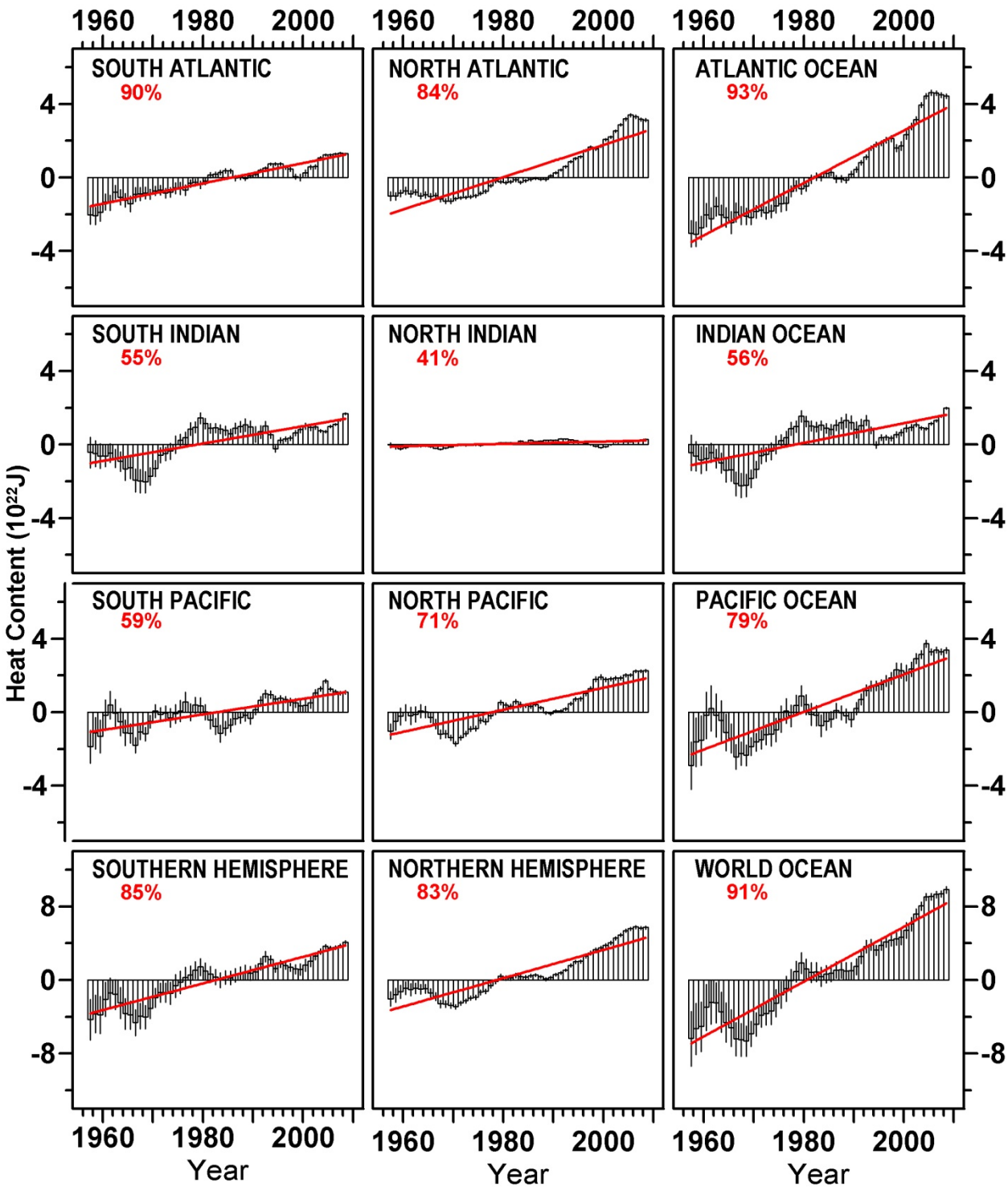

Figure S2. Time series of ocean heat content (10^{22}J) for the 0-700 m layer for the major ocean basins based on running pentadal analyses. Each pentadal estimate is plotted at the midpoint of the 5-year period. The vertical bars represent +/- 2.*S.E. about the pentadal estimate. The linear trend line and the percent variance accounted for by the linear trend are shown in red on each panel. Reference period is 1955-2006.

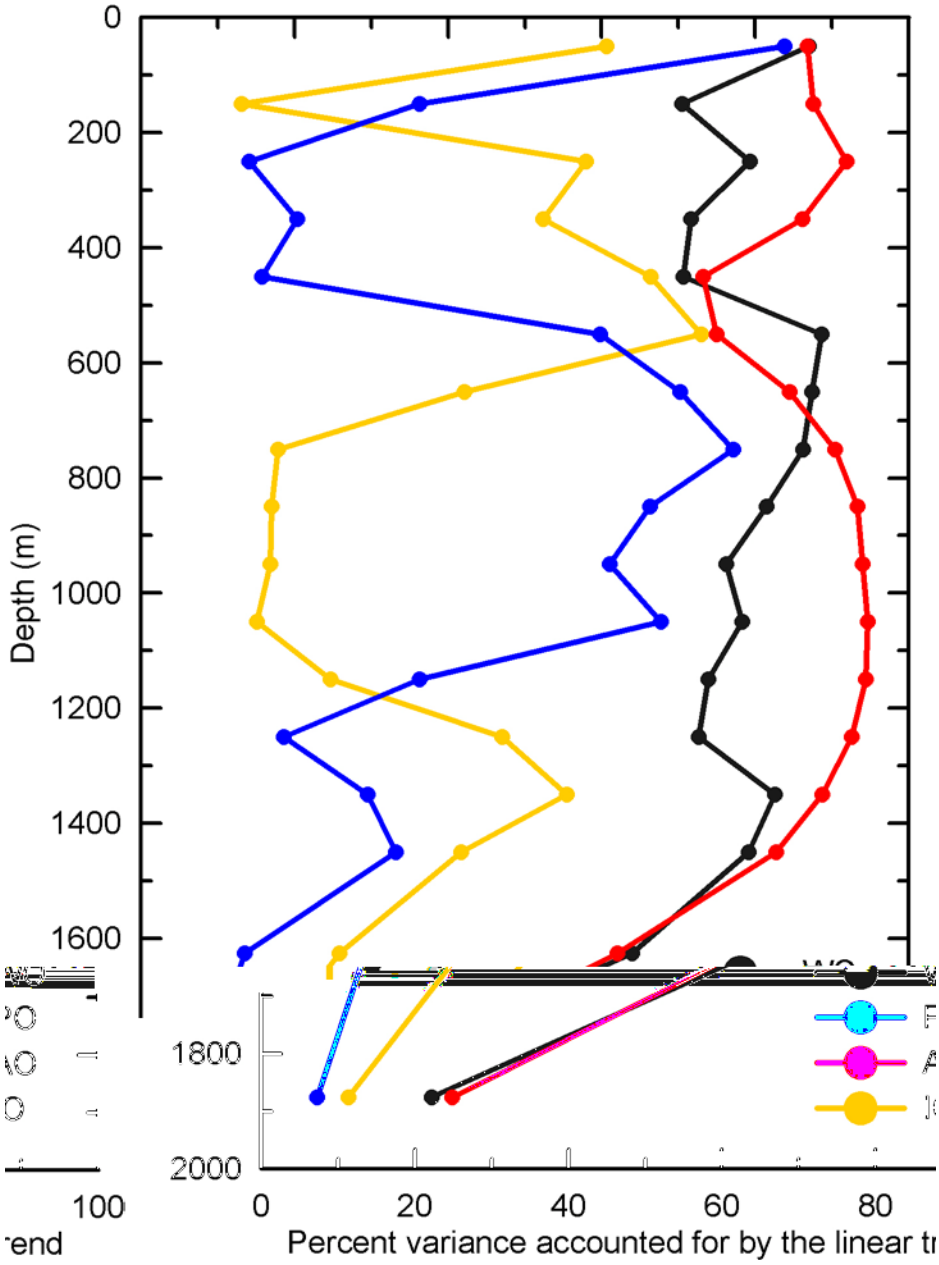

Figure S3. Percent variance accounted for by the linear trend of ocean heat content by 100 m-layers (Figure 2) for 1955-2010 by individual ocean basins.

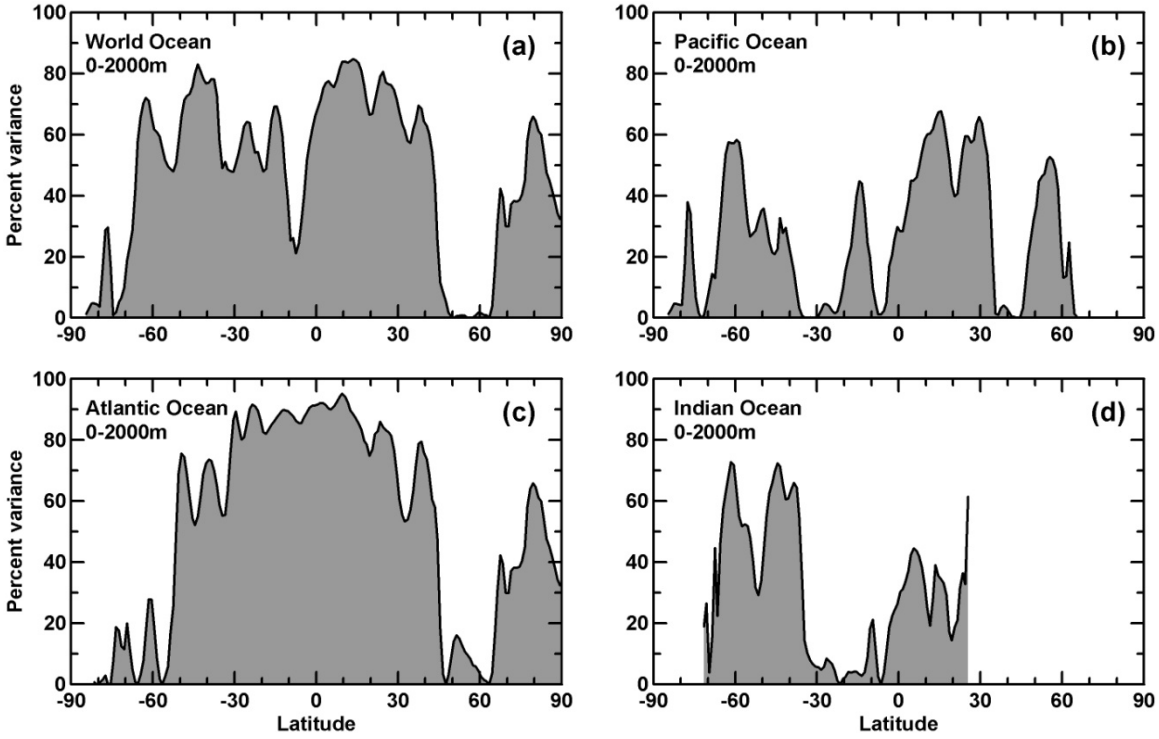

Figure S4. Percent variance accounted for by the linear trend of zonally integrated ocean heat content (0-2000 m layer) (figure 3) as a function of latitude for individual ocean basins.

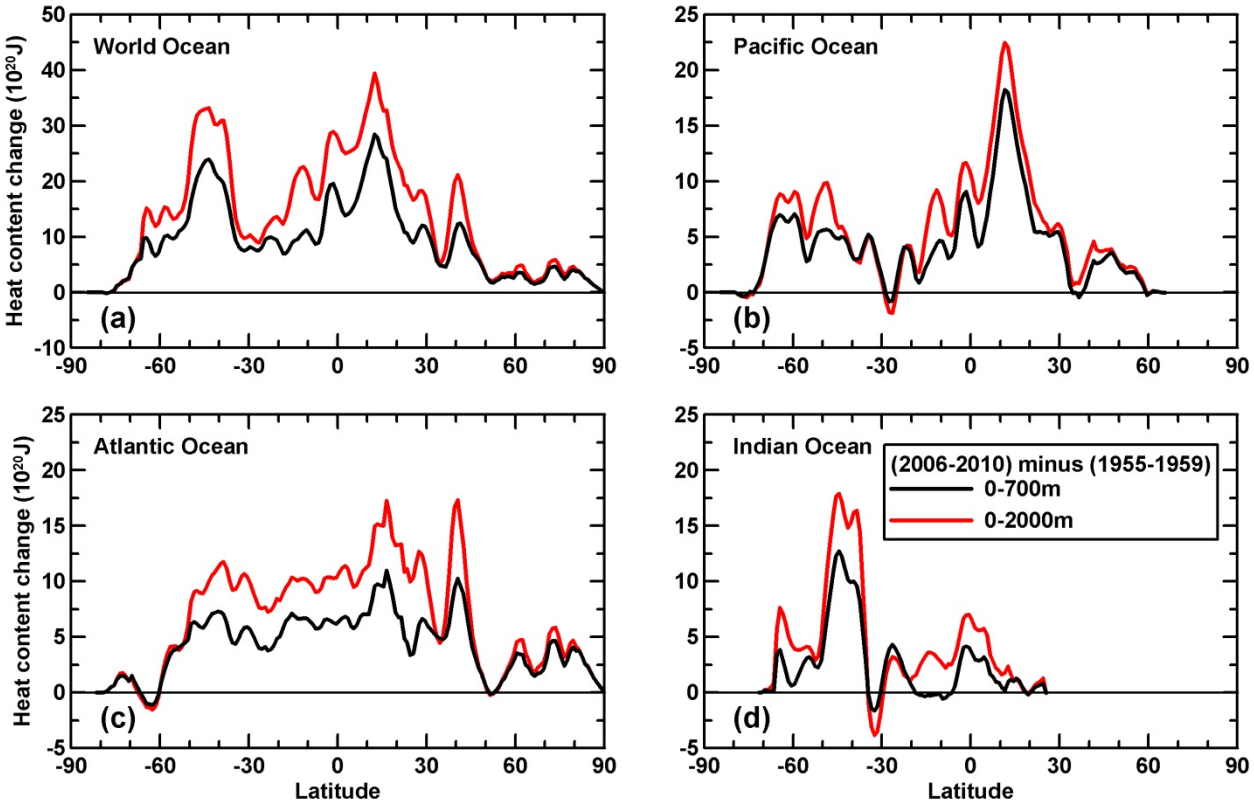

Figure S5. Zonal integral of the difference (2006-2010) minus (1955-1959) in OHC700 and OHC2000 for the World, Pacific, Atlantic, and Indian Oceans as function of latitude. Units of both curves are 10^{20} J.

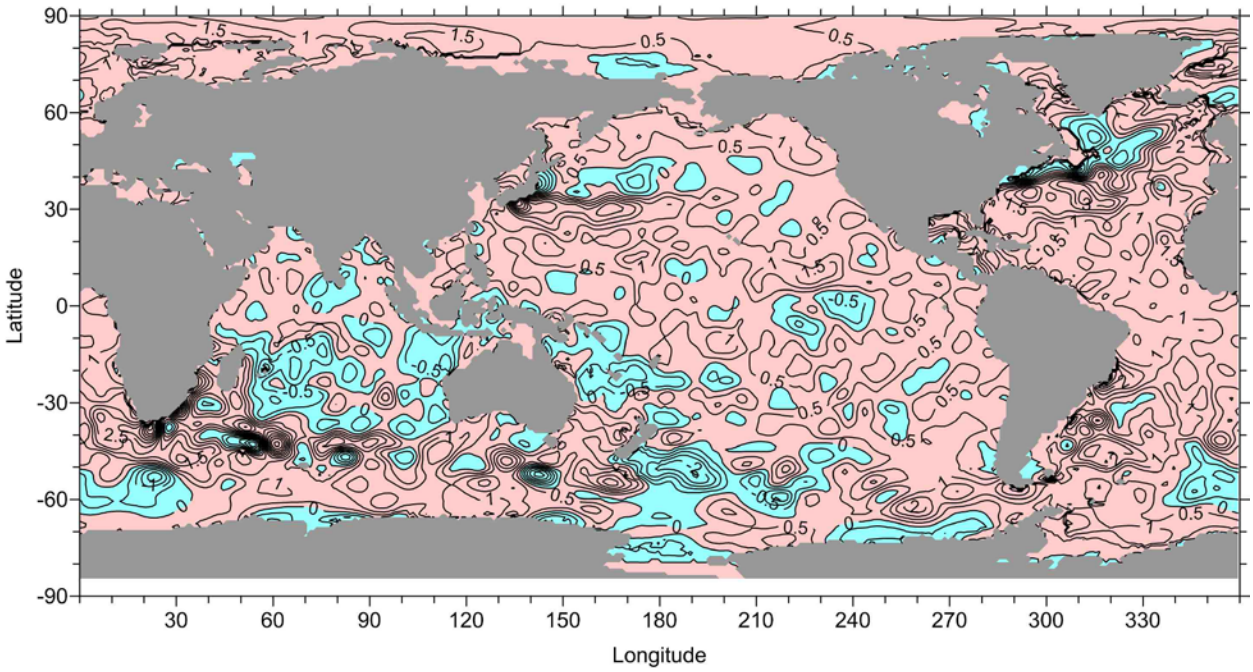

Figure S6. Linear trend of global geographic heat storage (Wm^{-2}) for the World Ocean for the 0-2000m layer.

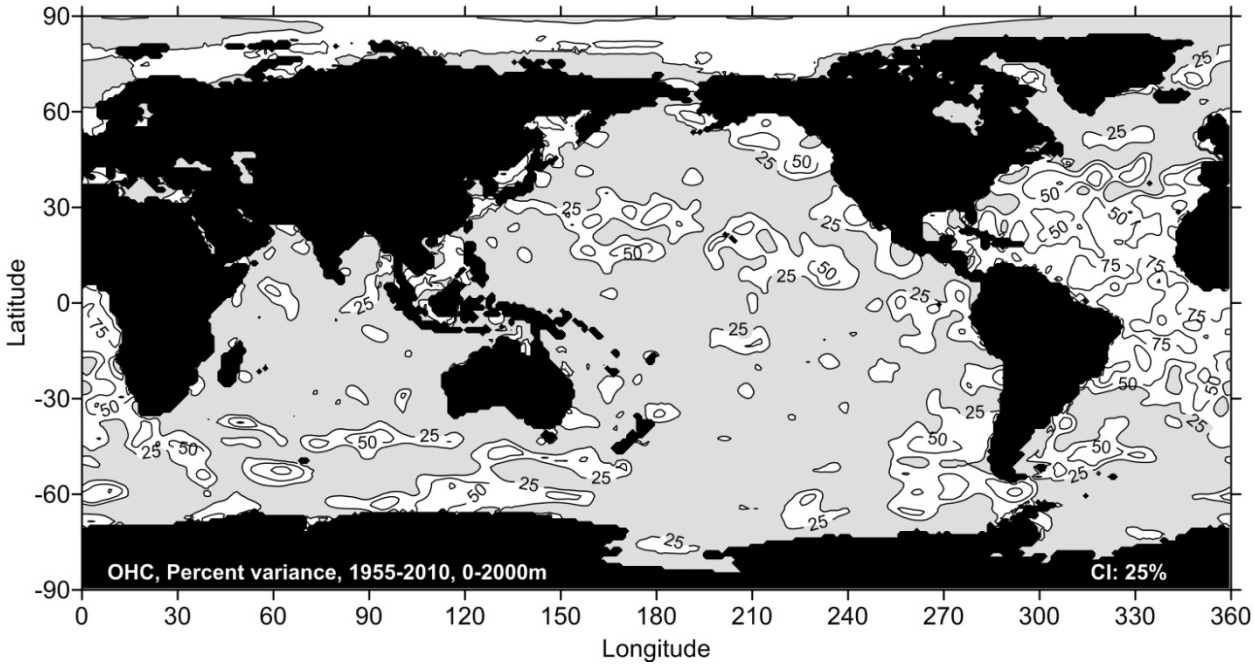

Figure S7. Percent variance accounted for by the linear trend of ocean heat content (0-2000 m layer) shown in figure S6.

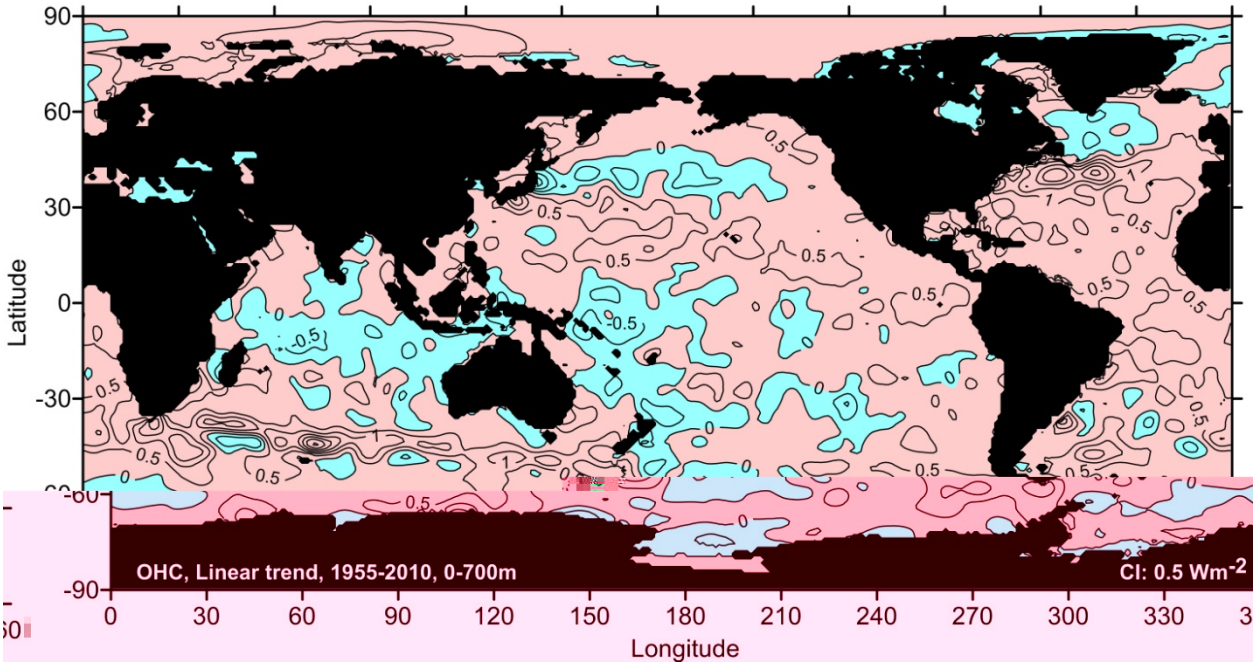

Figure S8. Linear trend of global geographic heat storage (Wm^{-2}) for the World Ocean for the 0-700m layer.

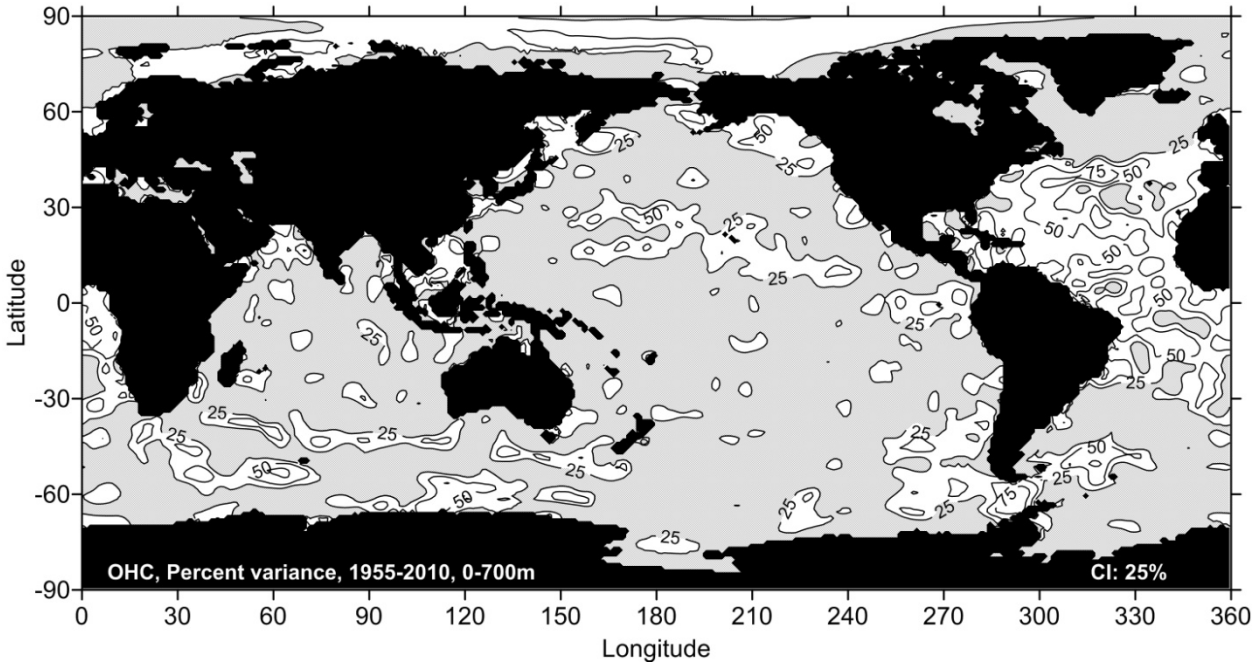

Figure S9. Percent variance accounted for by the linear trend of ocean heat content (0-700 m layer) (figure S8).

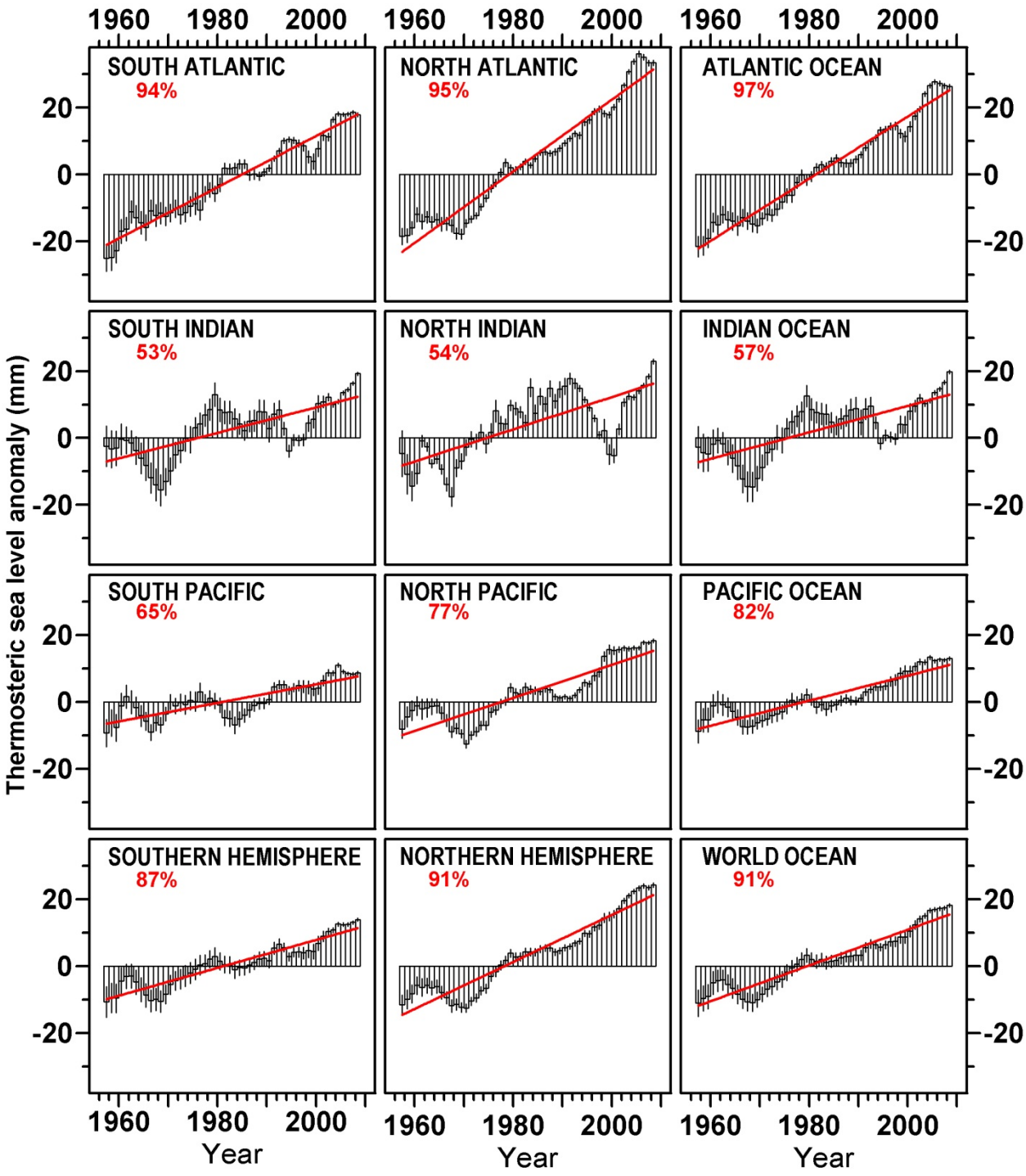

Figure S10. Time series of the thermosteric component of sea level trend mm yr^{-1} (0-2000 m layer) for the major ocean basins based on running pentadal analyses. Each pentadal estimate is plotted at the midpoint of the 5-year period. The vertical bars represent +/- 2.*S.E. about the pentadal estimate. The linear trend line and the percent variance accounted for by the linear trend is shown in red on each panel. Reference period is 1955-2006.

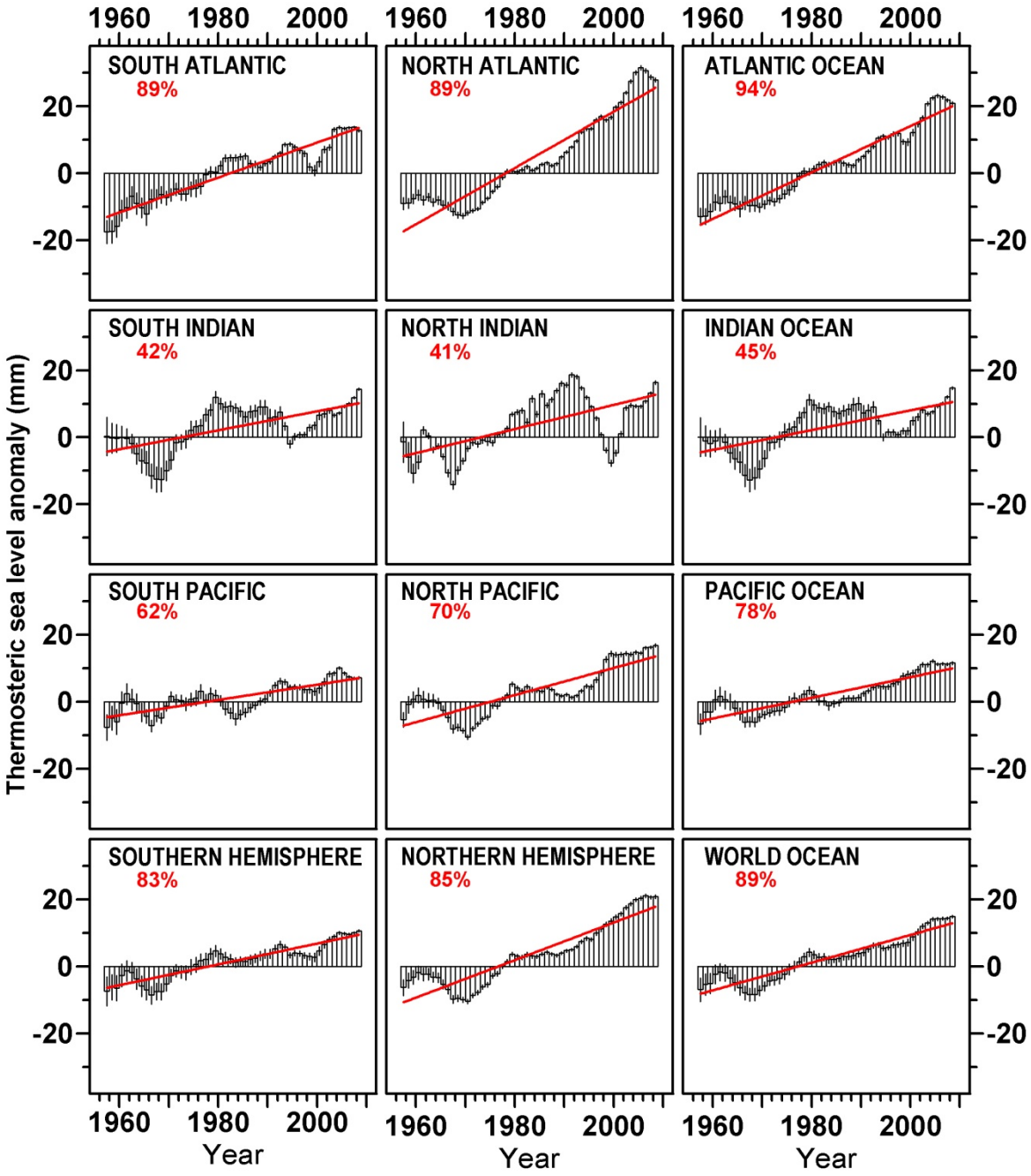

Figure S11. Time series of the thermosteric component of sea level trend mm yr^{-1} (0-700 m layer) for the major ocean basins based on running pentadal analyses. Each pentadal estimate is plotted at the midpoint of the 5-year period. The vertical bars represent +/- 2.*S.E. about the pentadal estimate. The linear trend line and the percent variance accounted for by the linear trend is shown in red on each panel. Reference period is 1955-2006.

Figure S12. Distribution of all temperature observations used in this study at 700 m depth for the world ocean reproduced from *Locarnini et al.,* [2010] (statistics at all standard levels and various climatological averaging periods are available at http://www.nodc.noaa.gov/OC5/WOA09F/pr_woa09f.html).

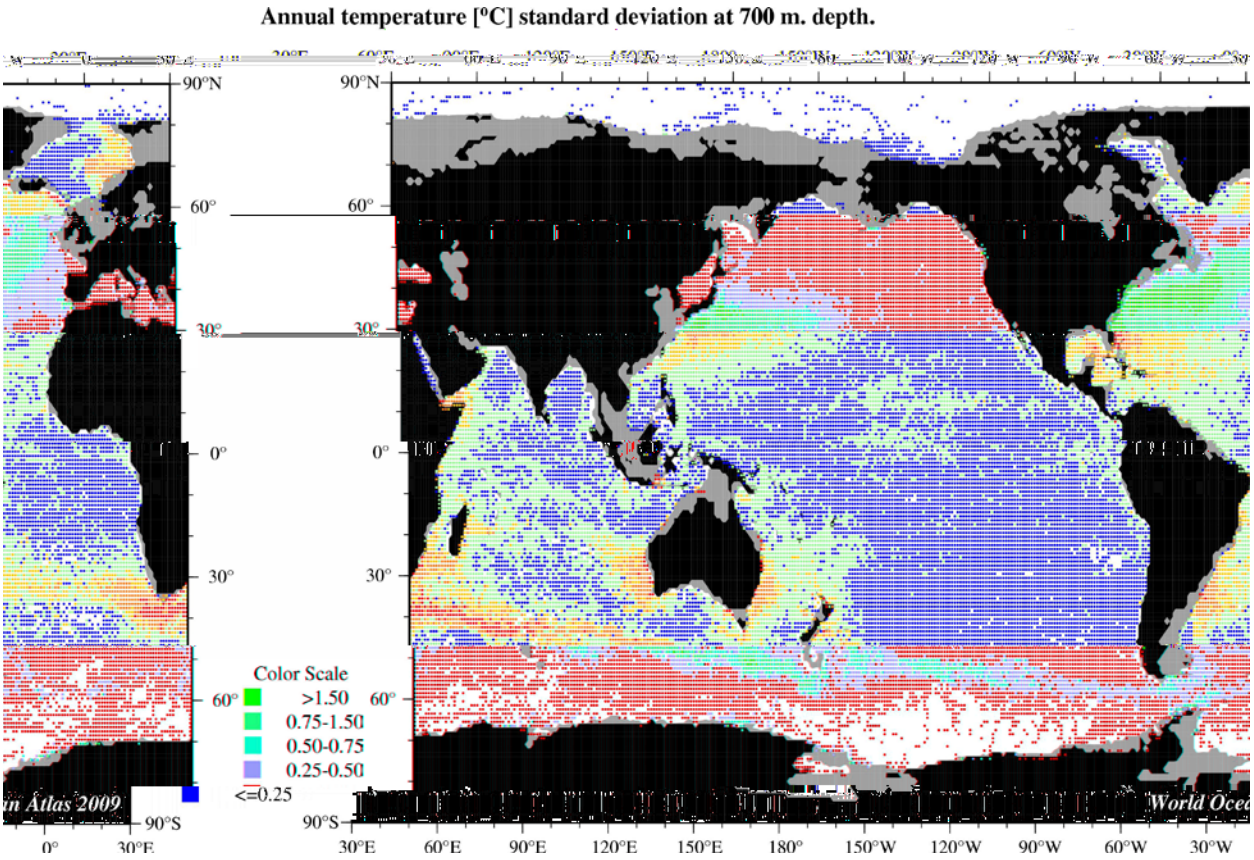

Figure S13. Distribution of the standard deviation of all temperature observations used in this study at 700 m depth for the world ocean reproduced from *Locarnini et al.* [2010] (statistics at all standard levels and various climatological averaging periods are available at http://www.nodc.noaa.gov/OC5/WOA09F/pr_woa09f.html).

Figure S14. Distribution of all temperature observations used in this study at 1750 m depth for the world ocean reproduced from *Locarnini et al.,* [2010] (statistics at all standard levels and various climatological averaging periods are available at http://www.nodc.noaa.gov/OC5/WOA09F/pr_woa09f.html).

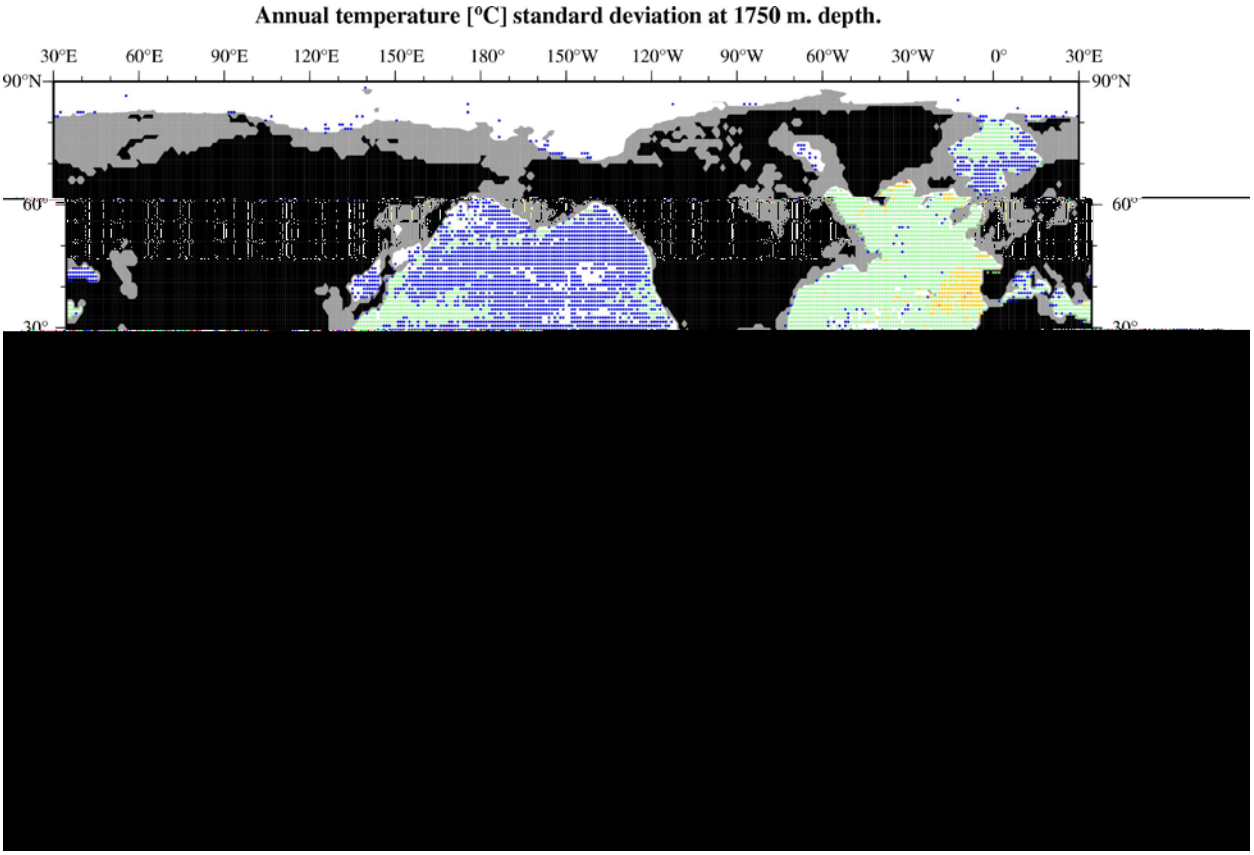

Figure S15. Distribution of the standard deviation of all temperature observations used in this study at 1750 m depth for the world ocean reproduced from *Locarnini et al.*, [2010] (statistics at all standard levels and various climatological averaging periods are available at http://www.nodc.noaa.gov/OC5/WOA09F/pr_woa09f.html).

Supplement Tables

Table S1. Tabular values of change in ocean heat content, volume mean temperature and related quantities for the 0-2000 m layer for the World Ocean and individual basins as determined by the linear trend for the 1955-2010 period. Heat storage is per unit area of each individual ocean basin surface.

Ocean Basin	HTrend	%VAR	HStorage	HChange	TChange
World Ocean	0.43	93.0	0.39	24.0	0.09
N. Hem.	0.21	92.0	0.47	11.9	0.11
S. Hem.	0.22	89.0	0.34	12.1	0.08
Atlantic	0.21	96.0	0.68	11.8	0.17
N. Atl.	0.12	94.0	0.73	6.7	0.19
S. Atl.	0.09	94.0	0.63	5.0	0.15
Pacific	0.14	84.0	0.25	7.9	0.06
N. Pac.	0.08	80.0	0.33	4.6	0.08
S. Pac.	0.06	64.0	0.19	3.3	0.04
Indian	0.08	68.0	0.34	4.3	0.08
N. Ind.	0.01	58.0	0.29	0.6	0.07
S. Ind.	0.07	65.0	0.34	3.8	0.08

Htrend – the linear trend [10^{22} J(year)$^{-1}$]
%Var – the percent variance accounted for by the linear trend
HStorage – heat storage [Wm^{-2}]
HChange – total change in heat content [10^{22} J]
TChange – total change in volume mean temperature [^{o}C]

Table S2. Tabular values of change in ocean heat content, volume mean temperature and related quantities for the 0-700 m layer for the World Ocean and individual basins as determined by the linear trend for the 1955-2010 period. Heat storage is per unit area of each individual ocean basin surface.

Ocean Basin	HTrend	%VAR	HStorage	HChange	TChange
World Ocean	0.30	91.0	0.27	16.7	0.18
N. Hem.	0.15	83.0	0.34	8.6	0.23
S. Hem.	0.15	85.0	0.23	8.1	0.14
Atlantic	0.14	93.0	0.46	8.0	0.31
N. Atl.	0.09	84.0	0.53	4.9	0.37
S. Atl.	0.06	90.0	0.39	3.1	0.25
Pacific	0.10	79.0	0.19	5.7	0.12
N. Pac.	0.06	71.0	0.24	3.4	0.16
S. Pac.	0.04	59.0	0.14	2.4	0.09
Indian	0.05	56.0	0.23	3.0	0.15
N. Ind.	0.01	41.0	0.19	0.4	0.12
S. Ind.	0.05	55.0	0.24	2.7	0.15

Htrend – the linear trend [10^{22} J(year)$^{-1}$]
%Var – the percent variance accounted for by the linear trend
HStorage – heat storage [Wm^{-2}]
HChange – total change in heat content [10^{22} J]
TChange – total change in volume mean temperature [^{o}C]

Table S3. Tabular values of the thermosteric component of sea level change for the 0-2000m and 0-700m layers for the World Ocean and individual basins as determined by the linear trend for the 1955-2010 period.

Ocean Basin	TH2000	%VAR2000	Change2000	TH700	%VAR700	Change700
World Ocean	0.54	91.0	30.0	0.41	89.0	23.2
N. Hem.	0.70	91.0	39.4	0.56	85.0	31.4
S. Hem.	0.42	87.0	23.4	0.31	83.0	17.4
Atlantic	0.93	97.0	52.1	0.69	94.0	38.8
N. Atl.	1.07	95.0	60.0	0.84	89.0	47.1
S. Atl.	0.77	94.0	42.9	0.52	89.0	29.2
Pacific	0.38	82.0	21.0	0.31	78.0	17.3
N. Pac.	0.49	77.0	27.6	0.41	70.0	22.7
S. Pac.	0.28	65.0	15.5	0.23	62.0	12.9
Indian	0.40	57.0	22.2	0.30	45.0	16.5
N. Ind.	0.48	54.0	27.0	0.36	41.0	20.1
S. Ind.	0.38	53.0	21.3	0.28	42.0	15.9

TH2000 – the linear trend [mm(year)$^{-1}$] for the 0-2000m layer
%Var2000 – the percent variance accounted for by the linear trend for the 0-2000m layer
Change2000 – total change in sea level [mm] due to thermal expansion of the 0-2000m layer
TH700 – the linear trend [mm(year)$^{-1}$] for the 0-700m layer
%Var700 – the percent variance accounted for by the linear trend for the 0-700m layer
Change700 – total change in sea level [mm] due to thermal expansion of the 0-700m layer

Auxiliary material

Appendix: Error Estimates of Objectively Analyzed Oceanographic Data

The results describing the variability of ocean heat content shown here are based on gridded (1-degree latitude-longitude grid), interpolated fields at standard depth measurement levels have statistical estimates of reliability associated with them. The objective analysis procedure used for interpolation is an iterative difference-correction method as described by *Levitus* [1982] and *Locarnini et al.* [2010]. In brief, the objective analysis scheme works as follows. At each standard depth level we first average all data within each 1° square (ODSQ) and subtract a first-guess value to produce a mean anomaly value. We define an "influence" region based on an influence radius, R, around each ODSQ, and compute a "correction" using all ODSQ values in the influence region based on a Gaussian-shaped, distance-related weight function. At each ODSQ the correction is added to the first-guess field to produce an "analyzed" value. Both the climatologies and anomaly fields produced in this way are characterized by a response function that shows that features with wavelength less than 555 km have been substantially (and deliberately) reduced in amplitude.

Mathematically at any gridpoint with coordinates (i,j) we compute an "analyzed" value as

$$A(i,j) = F(i,j) + C(i,j) \qquad (1)$$

in which

F(i,j) is a first-guess value for the gridpoint (i,j). As noted in the main text of this paper we used FG(i,j) = 0. in the anomaly computations presented here.

C(i,j) is a correction to the first-guess value and is defined as:

$$C(i,j) = \frac{\sum_{n=1}^{N} w_n Q_n}{\sum_{n=1}^{N} w_n} \qquad (2)$$

in which

N = is the total number of ODSQs containing data within the influence region surrounding the point (i,j)

Q_n = the difference between the observed ODSQ mean at gridpoint "n" and the first-guess value at this gridpoint so that $Q_n = (O_n - F_n)$. Each ODSQ mean anomaly value is based on all data values that occur within the ODSQ.

w_n = $\exp(-Er^2R^{-2})$ for $r \leq R$

w_n = 0 for $r > R$

r = distance of the n^{th} ODSQ within the influence region from the gridpoint (i,j) that

is being corrected.

E = 4.

Thus

$$C_{(i,j)} = \frac{w_1 Q_1}{W} + \frac{w_2 Q_2}{W} + ... + \frac{w_N Q_N}{W} \qquad (3)$$

in which

$$W = \sum_{n=1}^{N} w_n$$

The value W is just the sum of the weights within the influence region and for any particular data distribution is a constant for the influence region surrounding any gridpoint (i,j). The correction C(i,j) is simply a linear combination of all the corrections from within the influence region that are used to “correct” the first-guess value F(i,j).

We define

$$C_n = \frac{w_n Q_n}{W}$$

Next we estimate statistical errors of an objectively analyzed gridded field of oceanographic data. We apply a general formula for error propagation (GFEP) [*Taylor, 1997*] as follows. If an ODSQ analyzed value is $A(i,j) = \Sigma C_n$ (the first-guess value F(i,j) is a constant and we exclude it here), then its standard error (S.E.) according to GFEP is (we now drop the subscript from A(i,j))

$$\sigma_A = \sqrt{(\frac{\partial A}{\partial Q_1}\sigma_{C_1})^2 + ... + (\frac{\partial A}{\partial Q_N}\sigma_{C_N})^2 + 2\sum_{n=1}^{N-1}\sum_{m=n+1}^{N}(\frac{\partial A}{\partial Q_n})(\frac{\partial A}{\partial Q_m})\sigma_{C_{n,m}}} \qquad (4)$$

in which σ_{C_n} is the standard deviation of the anomaly values in the nth ODSQ within the influence region surrounding the gridpoint $A_{i,j}$ and $\sigma_{C_{n,m}}$ is the cross covariance between the nth and mth gridpoints containing data within the influence region.

Thus in our notation,

$$\sigma_A = \sqrt{(\frac{w_1}{W}\sigma_{C_1})^2 + ... + (\frac{w_N}{W}\sigma_{C_N})^2 + \frac{2}{W^2}\sum_{n=1}^{N-1}\sum_{m=n+1}^{N} w_n w_m \sigma_{C_{n,m}}} \qquad (5)$$

The problem we have in evaluating (5) is that the number of observations in each ODSQ may be from one observation in data sparse regions up to several hundred or more. Ideally, we would like to have a time series of measurements in each ODSQ with which we can produce statistics but this is simply not possible with the available data. Hence to evaluate standard deviations we will use the spatial variance of ODSQs containing data. Thus we compute the standard deviation

(σ_o) of all corrections C_n that are added to the first-guess field to produce the analyzed value A(i,j) after one pass of our objective analysis procedure with R = 666 km and γ = 0.8 (these values approximate the response function corresponding to the World Ocean Atlas 2001 [*Stephens et al., 2002*]three-pass analysis). The standard deviation (σ_o) of all observed ODSQ mean anomalies within the influence region surrounding an ODSQ at gridpoint (i,j) is defined as:

$$\sigma_0 = \sqrt{\frac{1}{N-1}\sum_{n=1}^{N}\left(C_n - \overline{C}_n\right)^2} \qquad (6)$$

in which $\bar{C}_n$ is the average of the "N" ODSQ anomalies that occur within the influence region.

The cross covariance $\sigma_{C_{n,m}}$ in (5) can be replaced by the quantity $\sigma_{C_n}\sigma_{C_m}$ because the Schwarz inequality guarantees that $\left|\sigma_{C_{n,m}}\right| \le \sigma_{C_n}\sigma_{C_m}$

Next we assume in equation (5) that $\sigma_{C_n} = \sigma_0$ and we have the standard error of the mean of the objectively analyzed value:

$$\sigma_A = \frac{\sigma_0}{W}\sqrt{\sum_{n=1}^{N} w_n^2 + 2\sum_{n=1}^{N-1}\sum_{m=n+1}^{N} w_n w_m} \qquad (7).$$

We document these statements by showing supplemental Figures S12 and S13 which are maps of the number of temperature observations and standard deviation of all temperature observations used in this study at 700m depth (from *Locarnini et al*. [2010]). Figures S14 and S15 show the

same statistics for 1750m depth. Examination of maps of the standard deviation demonstrate that this statistic is relatively homogenous and isotropic on the data averaging scales we use in our objective analyses for most of the world ocean.

2. Standard Deviation of Values Derived from ODSQ Analyzed Values

Having one-degree fields of σ_A simplifies the formal computation of the standard deviation of any value derived (SDDV) from the objectively analyzed fields, e.g., heat content. This is because we again use the general formula for error propagation. First, we calculate the partial derivatives (PD) of an equation used to compute any derived quantity based on our objectively analyzed field. Second, we multiply the PDs by the corresponding σ_A. Third, we add the squares of these products. The square root of this sum is the root-mean-square (RMS) error (or standard deviation) of the derived quantity.

There are two major assumptions for computing RMS error this way- all σ must be independent and random. If there are any doubts about these assumptions, a safer way is to estimate SDDV as follows [*Taylor, 1997*]. First, calculate the PDs. Second, multiply absolute values of the PDs by the corresponding σ_A. Third, add these products. This is an arithmetic sum of weighted σ_A (ASWS). In any case, RMS is never larger than ASWS.

For our error analysis, we compute standard errors as RMS if the derived quantity is a function of depth (i.e., for each individual ODSQ) and as ASWS if the derived variable is a function of longitude and/or latitude (i.e., for basin or zonal mean values).

References for Auxiliary Material

Levitus, S., 1982: *Climatological Atlas of the World Ocean*, NOAA Professional Paper No. 13, U.S. Gov. Printing Office, Wash., D.C., 173 pp., w/microfiche attachments.

Locarnini, R. A., A. V. Mishonov, J. I. Antonov, T. P. Boyer, and H. E. Garcia (2010), *World Ocean Atlas 2009, Volume 1: Temperature. NOAA Atlas NESDIS 68*, S. Levitus (Ed), U.S. Gov. Printing Office, Wash. D.C., 184 pp., (Available online at www.nodc.noaa.gov).

Stephens, C., J. I. Antonov, T. P. Boyer, M. E. Conkright, R. Locarnini, T. D. O'Brien, H. E. Garcia, 2002: *World Ocean Atlas 2001 Volume 1: Temperature*. S. Levitus, Ed., NOAA Atlas NESDIS 49, U.S. Gov. Printing Office, Wash., D.C., 168 pp., CD-ROMs.

Taylor, J. R. (1997), An Introduction to Error Analysis, 2nd edition, Sausalito, CA. University Science Books, 327 pp.